Keyel et al., Testing the role of patch openness as a causal mechanism for apparent area sensitivity

Online Resource 1: Methods Addendum

Field Size

Mean field sizes were 6.0, 5.3, 3.5, 4.0, 4.1 ha in June, July, August, September, and October respectively. See Table S1-1 for field sizes and locations.

Table S1-1 Field sizes and locations

Name	Area (ha)	Town	GPS Location
Upper Browning[a]	1.87	Lincoln	42° 24’ 47”N 71° 17’ 53”W
Lower Browning[a]	2.35	Lincoln	42° 24’ 40”N 71° 18’ 00”W
Farm Meadow[a]	8.10	Lincoln	42° 25’ 12”N 71° 19’ 39”W
Bobolink Field, Drumlin Farm[b]	2.37	Lincoln	42° 24’ 16”N 71° 19’ 49”W
Walden Pond State Park[c]	3.20	Concord	42° 25’ 50”N 71° 20’ 13”W
Clark Conservation Area[a]	4.09	Bedford	42° 29’ 24”N 71° 18’ 38”W
Little Meadow[a]	1.98	Bedford	42° 29’ 30”N 71° 18’ 50”W
Lake Wampanoag[b]	6.78	Gardner	42° 36’ 32”N 71° 58’ 01”W
High Ridge 1[d]	5.79	Gardner	42° 34’ 20”N 71° 55’ 51”W
High Ridge 2[d]	5.72	Gardner	42° 34’ 29”N 71° 55’ 32”W
High Ridge 3[d]	0.71	Gardner	42° 34’ 25”N 71° 55’ 36”W
High Ridge 4[d]	1.73	Gardner	42° 34’ 26”N 71° 55’ 28”W
High Ridge 5[d]	1.59	Gardner	42° 34’ 11”N 71° 55’ 47”W
High Ridge 6[d]	4.21	Gardner	42° 34’ 25”N 71° 55’ 50”W
High Ridge Smith St.[d]	3.14	Gardner	42° 35’ 18”N 71° 56’ 34”W
North Mowing, Wachusett Meadow[b]	4.16	Princeton	42° 27’ 25”N 71° 54’ 20”W
South East Mowing, Wachusett Meadow[b]	1.24	Princeton	42° 27’ 22”N 71° 53’ 56”W
Otter field, Wachusett Meadow[b]	0.93	Princeton	42° 27’ 28”N 71° 53’ 55”W
2nd Pasture, Wachusett Meadow[b]	1.09	Princeton	42° 27’ 15”N 71° 54’ 36”W
Rock Pasture, Wachusett Meadow[b]	0.84	Princeton	42° 27’ 16”N 71° 54’ 40”W
Field at Houghton Rd.[e]	5.71	Princeton	42° 27’ 35”N 71° 49’ 54”W
Field at Malden St.[e]	6.13	Holden	42° 21’ 47”N 71° 49’ 20”W
Field near Sterling Rd. and Mason Rd.[e]	9.46	Holden	42° 24’ 52”N 71° 51’ 26”W
Oxbow NWR field 1[f]	9.69	Harvard	42° 29’ 33”N 71° 37’ 18”W
Oxbow NWR field 2[f]	7.76	Harvard	42° 29’ 44”N 71°36’57”W
Assabet River NWR Drop Zone[f]	10.62	Maynard	42° 24’ 43”N 71° 28’ 29”W
30W field [g]	17.85	North Grafton	42° 15’ 05”N 71° 40’ 18”W
Yorkshire Ln field[g]	2.86	North Grafton	42° 14’ 20”N 71° 41’ 15”W

Name	Area (ha)	Town	GPS Location
Moose Hill large field [d]	7.27	Spencer	42° 17’ 00”N 71° 58’ 01”W
Moose Hill small field [d]	0.95	Spencer	42° 16’ 59”N 71° 57’ 52”W
Moore State Park large field[c]	10.17	Paxton	42° 18’ 39”N 71° 57’ 05”W
Moore State Park small field 1[c]	1.70	Paxton	42° 18’ 50”N 71° 56’ 54”W
Moore State Park small field 2[c]	1.05	Paxton	42° 18’ 52”N 71° 56’ 51”W
Moore State Park small field 3[c]	0.88	Paxton	42° 18’ 54”N 71° 56’ 49”W
Moore State Park field 4[c]	3.02	Paxton	42° 18’ 56”N 71° 56’ 39”W
Appleton Farm Broad Meadow [h]	18.02	Ipswich	42° 39’ 02”N 70° 50’ 47”W
Appleton Farm Great Pasture [h]	48.98	Ipswich	42° 38’ 45”N 70° 51’ 36”W
Old Town Hill Field 12 [h]	1.96	Newbury	42° 46’ 03”N 70° 51’ 38”W
Old Town Hill Field 222 [h]	4.24	Newbury	42° 46’ 25”N 70° 51’ 31”W
Woodsom Farm North field[a]	29.26	Amesbury	42° 51’ 51”N 70° 57’ 28”W
Woodsom Farm South field[a]	18.91	Amesbury	42° 51’ 31”N 70° 57’ 28”W
Nichols Brook Conservation Area[a]	5.58	Middleton	42° 36’ 58”N 70° 59’ 08”W
Charles River Penninsula [h]	7.41	Needham	42° 15’ 28”N 71° 16’ 03”W
Brookwood Farm field 1[c]	0.60	Milton	42° 12’ 25”N 71° 06’ 44”W
Brookwood Farm field 2[c]	1.45	Milton	42° 12’ 19”N 71° 06’ 37”W
Brookwood Farm field 3[c]	2.03	Milton	42° 12’ 24”N 71° 06’ 36”W
Brookwood Farm field 4[c]	1.23	Milton	42° 12’ 27”N 71° 06’ 32”W
Brookwood Farm field 5[c]	1.36	Milton	42° 12’ 22”N 71° 06’ 24”W

[a]Town Conservation Land, [b]Massachusetts Audubon Society Sanctuary, [c]Massachusetts Department of Conservation and Recreation (DCR) State Park, [d]Massachusetts Wildlife Management Area, [e]DCR Public Water Supply Land, [f]Eastern Massachusetts National Wildlife Refuge Complex, [g]Tufts Cummings School of Veterinary Medicine, [h]The Trustees of Reservations

Distance Sampling

We compared uniform, half-normal and hazard rate key functions using AIC, and selected the uniform key function with one cosine adjustment term (Fig S1-1). Choice of model did not strongly influence the density estimates. The model was constrained to be strictly monotonic, non-increasing. When more than one bobolink was observed together, we recorded them as a cluster, and we used mean of cluster size in our density estimates, as we had too few clusters with size >1 to justify using size-biased regression.

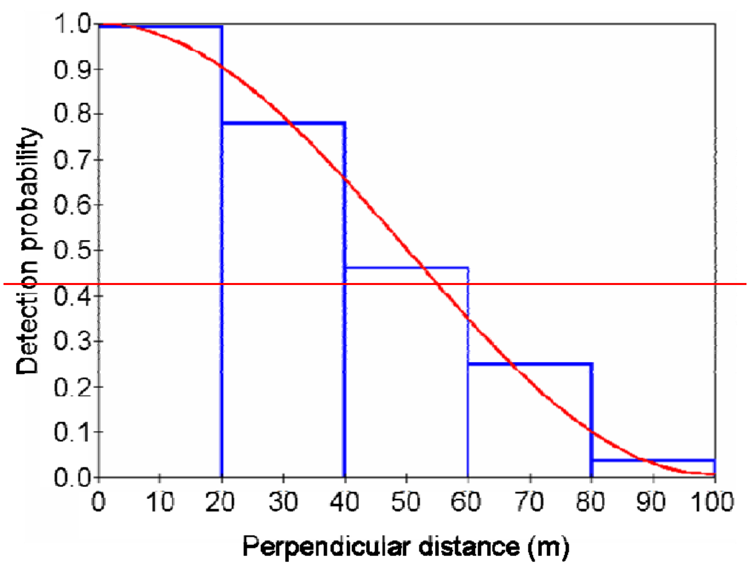

Fig. S1-1 Pooled detection function for male Bobolinks based on 43 sites and 142 Bobolink observations.

Edge Effects Model

The edge effects model (EEM) was computed using ArcInfo 9.3. All surrounding edges of each site were digitized and classified as one of 8 edge types (Table S1-2). Buffers were generated at 75 and 150 m, and any area inside the field not covered by the buffers was digitized as an additional polygon. These buffer sizes are specific to bobolinks, and coincide with empirical observations of densities (Fletcher and Koford 2003). Buffers were used to create a series of polygons that had the edge discounts for each edge affecting that polygon; no discount was applied to interior polygons. These discounts were multiplied by the area of each part, to give an overall abundance for that part. The part abundances were then summed for the entire field, and divided by total field area to get an estimate of average whole field density. See Fig. S1-2 for an illustrative example.

We made several assumptions in our edge effects model. 1. Edge responses measured by Fletcher and Koford (2003) in Iowa applied to edges in Massachusetts. 2. Our edge generalizations from Fletcher and Koford (2003) were valid, and that our values for unmeasured edge types were sufficiently accurate. 3. Edge effects were multiplicative. We made this assumption because Fletcher (2005) showed a 50% reduction next to one edge, and a further 50% reduction next to a second edge. Fletcher only examined this in the context of 2 agricultural edges; we extrapolated from this pattern for all edge types and to any number of edges. 4. Edges on the interior of a site (e.g., a small island of woods in a field) had the same effect as edges on the exterior perimeter of the site. 5. Edges only affected portions of the field perpendicularly from that edge. Specifically, we did not allow overlapping effects from edges of different types on the same side (Fig. S1-3). 6. This method was designed for a rectangular field. We assumed that the approximations required to apply it to non-rectangular fields were valid.

Table S1-2 Discount values for the edge effects model. Values in the table represent the percent reduction in bird density for areas falling within that buffer distance. Wetland, shrub, and "other" values made up very little of the edge cover in our study area.

Distance (m)	Agriculture[a]	Road[a]	Woodland[a]	Structure/ Residential[b,c]	Wooded Road[b,d]	Wetland[b,e]	Shrub[b,f]	Other
0-75	0.7	0.6	0.5	0.5	0.4	0.8	0.6	Case by
76-150	1.0	1.0	0.8	0.8	0.8	1.0	1.0	Case

[a] Discount values for agriculture, road and woodland were approximated based on figure 2 of Fletcher and Koford 2003.
[b] We could not find data for other edge types, but decided a best guess would be more realistic than applying no edge reduction at all.
[c] As our residential areas tended to be wooded, we used the same discount as for woodland.
[d] For wooded roads, we decided that that the combination was likely worse than either woods or road alone, so we allowed a slightly larger discount.
[e] We decided wetlands were likely to have less effect on bobolinks than would agriculture, so we discounted them less.
[f] The Shrub discount was arbitrarily selected to be somewhat smaller than that for woodland, but worse than for agriculture

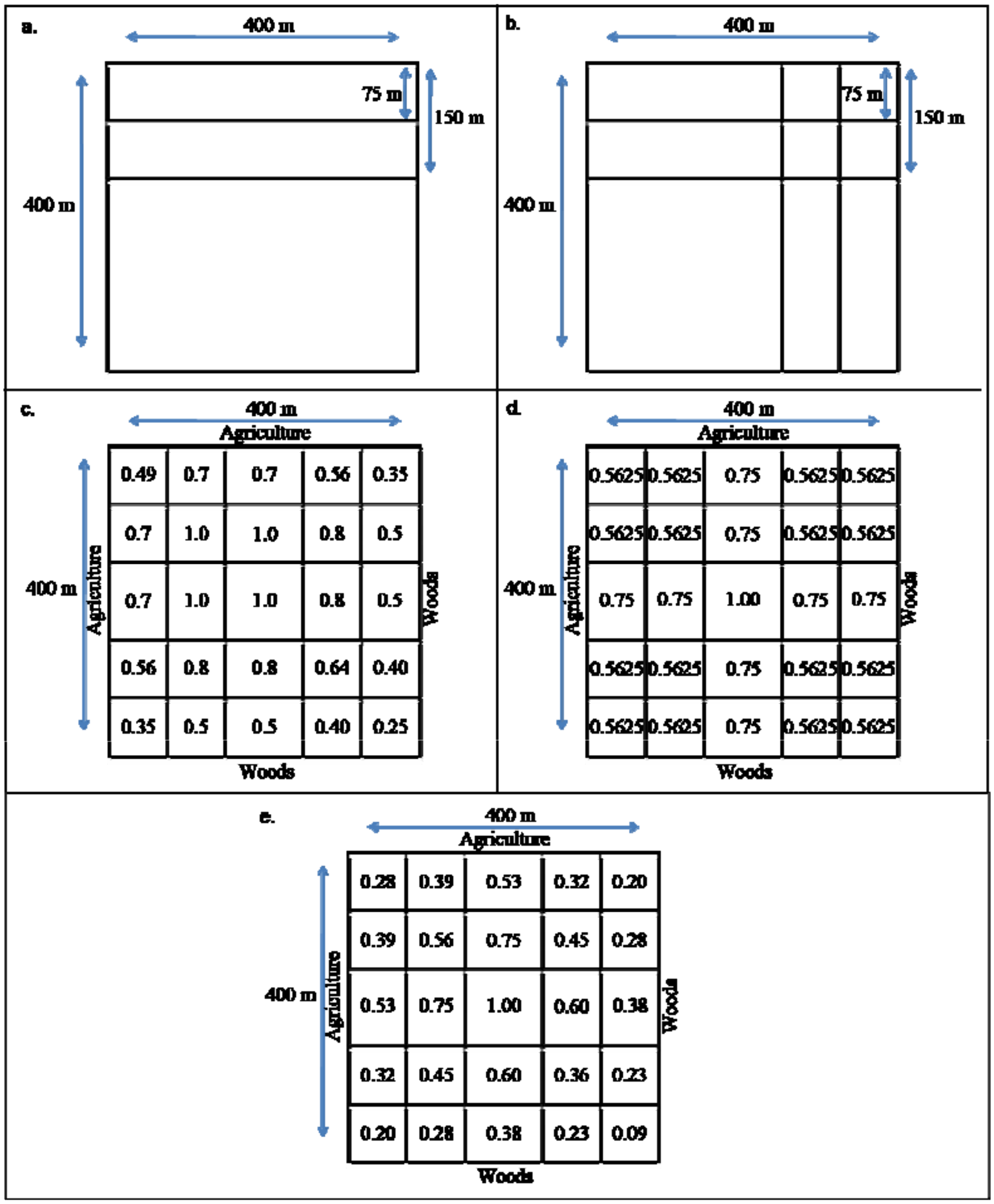

Fig. S1-2 An example illustrating the edge effects model (EEM) using a hypothetical field 400 m x 400 m bordered by woods and agriculture. a) depicts the field with 75 m and 150 m buffers from the top edge. b) shows the overlap of buffers depicted for the top edge and the right edge. c) depicts buffers for all four edges. Numbers in each cell are the standardized densities discounted based on edge effects, and they coincide with values from Table S1-2. Note that if there were no edge effects, all polygons would be 1.0. When buffers overlap, the polygon discount (cell value) is the product of buffer discount values. In the center, proportional (standardized) density is 1.0, because no edge buffers overlap this area. In the bottom center, density is 0.50, because this is within 75 m (0.5 reduction) of one wooded edge. The top right corner density is 0.35, because it is affected by the 75 m buffers from both the wooded edge and the agricultural edge. d) The numbers in the polygons are the areas (ha). The middle area is 100 m x 100 m, the bottom center is 100m x 75m, and the top right is 75m x 75m. Total area is 16 ha. e) shows the estimated abundances for each part. This is equal to density (c) times area (d). The estimated density is the sum of the cells (10.56) / total area(16); in our example, the estimated density is 0.66 bobolinks / ha instead of 1 bobolink/ha.

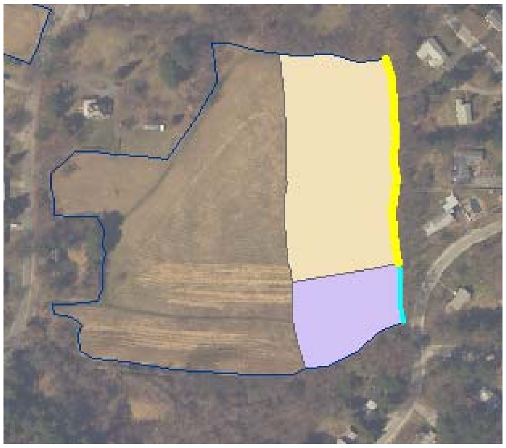

Fig. S1-3 A partial example (just depicting one side of a patch) of how buffers were applied in the effective area model. The edge in yellow is one edge type (wooded) and the edge in blue is a second edge type (wooded road). The two edge effects (beige and purple polygons, respectively) do not overlap since they are on the same edge of the field. One concern with this approach is that a particularly negative edge type may be more influential than a more benign edge type.

Openness Measures

We examined 11 measures of openness. We laid down a transect along the long axis of each site (field), with points at one end of the transect on the field edge, then every 50 m, and a final point at the terminus of the transect, at the field edge. In addition to the transect points, another point was taken at the most open point in the field (visually estimated in the field). Data were collected at each point using an inclinometer, and with a Solar Pathfinder (http://www.solarpathfinder.com/). The Solar Pathfinder is a convex lens that reflects the nearby horizon. We took 2 photographs of the Solar Pathfinder image (because half the image is obscured by the observer) and orthorectified them with Pathfinder Assistant 4.0. The images were then exported to Image J (Rasband 2009) and combined to get an overall measure of openness at the point. We analyzed both inclinometer and Solar Pathfinder data in 5 different ways: 1) the full transect, 2) excluding transect points within 50 m from the edge, 3) only the starting and ending transect points, 4) the full transect weighted by the width of the field at that point, and 5) using only the single most open point of the site (i.e. where the angle readings were lowest; could be off transect). Since these measures were collected with both the Solar Pathfinder and the inclinometer, this gave us 10 different measures of openness. We also measured "open area," defined as the amount of area in a site with less than a 27.5º angle to the horizon. We chose this angle because all points <27.5º receive full sun even in December (based on field measurement with the Solar Pathfinder, unpubl. data). Based on 14 sites, inclinometer measures were superior to measurements taken with the Solar Pathfinder (Table S1-3) including the open area approach, so no further measurements were taken with the Solar Pathfinder. Of the 5 remaining measurements, the edge-only measurements were very poor predictors of Bobolink density and were dropped. The weighted transect measurement was slightly worse or equivalent to the other remaining measurements and was dropped as it required more effort to calculate. This left us with 3 suitable and correlated ($R^2 > 0.81$) measurements of openness, of which we decided to use the full transect, as this measure could still be used at very small sites, unlike the transect without edge points. It was also slightly better at predicting Bobolink density than was the most open point.

Table S1-3 Relationship between openness measures and Bobolink density (#/ha) at a subset of sites (n = 14). See text for details.

Variable	r	P
1. Inclinometer, full transect	-0.55	0.04
2. Inclinometer, transect, no edge points	-0.60	0.02
3. Inclinometer, edge points only	-0.33	0.25
4. Inclinometer, weighted transect	-0.53	0.05
5. Inclinometer, most open point	-0.53	0.05
6. Pathfinder, full transect	0.41	0.14
7. Pathfinder, transect, no edge points	0.46	0.10
8. Pathfinder, edge points only	0.13	0.65
9. Pathfinder, weighted transect	0.38	0.18
10. Pathfinder, most open point	0.50	0.07
11. Open Area	0.44	0.12

Body Condition - CORT Methods

A baseline blood sample was taken within 3 min of a bird hitting the net (Romero and Reed 2005). Additional blood samples were taken after 20 and 110 min. An ACTH injection (100 IU/kg b.w.) was given after the 110 min blood sample to determine the capacity of the bird to secrete corticosterone (CORT), and a final blood sample was taken 15 min later. All blood samples were taken from the brachial vein and collected in heparinized capillary tubes. Bleeding was staunched with cotton. Total blood volume taken did not exceed 1% of the bird's body weight (Fair et al. 2010). Between blood samples, birds were banded and fat score, mass, and natural wing-chord measured; birds were otherwise held in opaque cloth bags. Fat score ranges from no fat visible (0) to fat bulging past the furculum (5) (Helms and Drury 1960); low fat scores (≤1) are typical for many species of birds during breeding (e.g., Romero et al. 1997.). All individuals sampled had low fat scores <1, and are not discussed further.

Blood samples were stored on ice for up to 8 h until centrifuged. After centrifugation, plasma was removed and stored at -20 C. We determined CORT concentrations in each sample using radioimmunoassay (RIA) following the methods of Wingfield et al. (1992). Briefly, samples were allowed to equilibrate overnight with a small amount of radiolabeled CORT to determine individual recoveries. CORT was extracted from each sample with 4 ml of dichloromethane, then samples were dried under nitrogen gas and re-suspended in phosphate-buffered saline with 1% gelatin. Tritiated CORT and CORT antibody (Endocrine Sciences, B3-163, Calabasas Hills, California, USA) were added to samples and standards and allowed to equilibrate. We added dextran-coated charcoal to adsorb unbound steroid, and separated bound from unbound fractions using centrifugation. The bound fraction was decanted, mixed with scintillation fluid and counted. Samples were assayed in duplicate, and assay values corrected for individual recoveries following extraction. Inter- and intra-assay coefficients of variation were determined by running standards in each assay. Intra-assay variation was 9.4%; inter-assay variation was 14.5%.

Online Resource 1 Literature Cited

Fair JM, Paul E, Jones J (2010) Guidelines to the use of wild birds in research. Washington, D.C.: Ornithological Council.

Fletcher RJ Jr, Koford RR (2003) Spatial responses of bobolinks (*Dolichonyx oryzivorus*) near different types of edges in Northern Iowa. Auk 120:799-810

Helms CW, Drury WH Jr. (1960) Winter and migratory weight and fat field studies on some North American buntings. Bird-Band 31: 1-40Rasband WS, (1997-2009) ImageJ, U. S. National Institutes of Health, Bethesda, Maryland, USA, http://rsb.info.nih.gov/ij/

Romero LM, Ramenofsky M, Wingfield JC (1997) Season and migration alter the corticosterone response to capture and handling in an arctic migrant, the White-crowned Sparrow (Zonotrichia leucophrys gambelii). Comp Biochem Physiol C 116:171-177

Romero LM, Reed JM (2005) Collecting baseline corticosterone samples in the field: Is under 3 min good enough? Comp Biochem Phys A 140:73-79

Wingfield JC, Vleck CM, Moore MC (1992) Seasonal changes of the adrenocortical response to stress in birds of the Sonoran Desert. J Exp Zool 264:419-428

Online Resource 2

Table S2-1 Table 1 addendum containing parameter estimates ± SE (below) for models. Non-significant equations are included as measures of effect size. Thresholds were 72.43°, 69.99°, 72.43°, 80.99° for June, July, August, and September respectively. Full model includes all variables. Models are presented by month ordered by logistic ΔAICc values (given in Table 1). β values correspond to the (arbitrary) order in which the variables are given and β_0 indicates the intercept. Variables for the full model are given in the order listed above. Full models are given on 2 lines, with the second line continuing with the 4th variable (TE).

		Logistic[a]				Linear			
Month	Model[b]	β_0	β_1	β_2	β_3	β_0	β_1	β_2	β_3
June	OI	-1.61	2.37	-	-	-6.82	0.11	-	-
		0.63	0.78			2.61	0.04		
n = 40	OI + A	-1.70	2.04	0.056	-	-5.48	0.087	0.038	-
		0.65	0.91	0.086		3.29	0.047	0.056	
	OI + EEM	-1.70	2.27	0.38	-	-4.74	0.071	1.49	-
		0.78	0.93	1.80		3.25	0.049	1.40	
	A	-1.11	0.19	-	-	0.55	0.34	-	-
		0.53	0.10			0.11	0.04		
	LA	-1.29	0.91	-	-	0.39	0.40	-	-
		0.59	0.40			0.60	0.27		
	TE	-1.51	1.21	-	-	0.18	0.83	-	-
		0.72	0.62			0.46	0.35		
	EEM	-1.49	3.19	-	-	-0.10	2.90	-	-
		0.73	1.66			0.48	1.02		
	Full	0.21	3.68	0.63	-1.09	-7.10	0.098	-0.09	-0.86
		1.74	1.60	0.40	1.53	3.96	0.060	0.21	0.75
		-	-2.33	-4.63	-	-	0.99	3.30	-
			2.42	4.68			1.53	2.86	
July	OI	-3.50[c]	4.16[c]	-	-	-10.15	0.16	-	-
		1.48	1.53			4.20	0.06		
n = 43	OI + A + EEM	-2.60[c]	4.20[c]	0.24[c]	-4.95[c]	-7.67	0.10	-0.14	5.88
		1.61	1.60	0.21	3.71	5.47	0.08	0.19	3.90
	OI + EEM	-3.08[c]	4.44[c]	-1.60[c]	-	-6.25	0.083	4.20	-
		1.58	1.60	2.27		5.11	0.080	3.18	
	OI + TE	-3.78[c]	3.83[c]	0.52[c]	-	-12.87	0.21	-1.02	-
		1.57	1.58	0.89		5.10	0.08	1.08	
	OI + TE + EEM	-3.37[c]	4.04[c]	1.18[c]	-3.16[c]	-9.17	0.14	-1.61	5.69
		1.60	1.58	1.14	2.79	5.42	0.09	1.11	3.30
	Full	-2.04[c]	3.75[c]	0.15[c]	0.84[c]	-8.66	0.15	0.29	0.17
		2.13	1.59	37	1.91	6.16	0.09	0.35	1.60
		-	-0.73[c]	-5.19[c]	-	-	-3.29	3.35	-
			2.55	4.39			2.65	4.66	
	LA	-1.79	1.34	-	-	0.40	0.93	-	-
		0.65	0.48			0.64	0.49		
	TE	-2.46	2.20	-	-	0.45	0.94	-	-
		0.87	0.83			0.91	0.84		
	A	-1.54	0.31	-	-	0.47	0.22	-	-
		0.59	0.13			0.62	0.12		
	EEM	-1.41	2.87	-	-	-1.07	6.51	-	-
		0.78	1.89			0.92	2.25		

		Logistic[a]				Linear			
Month	Model[b]	β_0	β_1	β_2	β_3	β_0	β_1	β_2	β_3
August	OI	-3.61[c]	3.72[c]	-	-	-7.36	0.11	-	-
		1.47	1.55			3.37	0.05		
n = 35	OI + LA	-3.35[c]	5.45[c]	-1.22[c]	-	-11.68	0.18	-0.74	-
		1.43	2.32	1.10		5.06	0.08	0.65	
	OI + A	-3.27[c]	4.72[c]	-0.24[c]	-	-12.90	0.20	-0.31	-
		1.50	1.83	0.22		4.51	0.07	0.18	
	OI + TE	-2.83[c]	4.72[c]	-1.39[c]	-	-8.42	0.13	-0.41	-
		1.64	1.89	1.43		4.46	0.07	1.09	
	OI + A + TE	-3.07[c]	4.78[c]	-0.17[c]	-0.50[c]	-12.10	0.18	-0.68	2.73
		1.69	1.89	0.34	2.15	4.41	0.07	0.28	1.64
	LA	-2.44	1.24	-	-	0.32	0.49	-	-
		0.86	0.58			0.52	0.42		
	TE	-2.80	1.76	-	-	-0.25	1.12	-	-
		1.04	0.90			0.76	0.75		
	Full	-3.23[c]	4.59[c]	-0.12[c]	-0.81[c]	-11.98	0.17	-0.77	-0.11
		2.05	2.42	0.66	2.94	4.98	0.08	0.42	1.46
		-	0.11[c]	1.34[c]	-	-	3.10	1.76	-
			2.54	4.76			2.07	3.84	
	A	-2.05	0.26	-	-	0.48	0.08	-	-
		0.73	0.15			0.57	0.13		
	EEM	-2.68	4.39	-	-	0.16	1.74	-	-
		1.06	2.54			0.84	2.22		
September	OI	-3.43[c]	5.38[c]	-	-	-0.81	0.012	-	-
		1.48	2.29			0.47	0.006		
n = 18	OI + A	-3.60[c]	4.63[c]	0.16[c]	-	-1.34	0.021	-0.037	-
		2.02	2.05	0.33		0.56	0.008	0.023	
	TE	-5.08	3.05	-	-	-0.01	0.09	-	-
		2.60	1.96			0.13	0.12		
	EEM	-3.75	5.21	-	-	-0.02	0.25	-	-
		1.88	3.96			0.13	0.33		
	LA	-2.93	1.01	-	-	0.051	0.024	-	-
		1.61	1.00			0.091	0.067		
	A	-2.45	0.19	-	-	0.066	0.003	-	-
		1.26	0.22			0.092	0.019		
	Full	-2.91[c]	3.49[c]	0.30[c]	-1.39[c]	-1.22	0.016	-0.064	-0.09
		4.07	2.61	1.08	3.29	0.68	0.012	0.068	0.22
		-	0.77[c]	0.78[c]	-	-	0.32	0.38	-
			6.52	9.44			0.38	0.59	

[a]Probability of absence was modeled. [b] Units are as follows: Openness (OI): unitless (logistic, binary variable before (0) or after (1) threshold), degrees (linear), Area (A): ha, Ln Area (LA): ln (ha), Total Edge (TE): km, Edge Effects Model (EEM) (standardized number/ha). [c]Due to the high model fit the maximum likelihood estimate was unreliable, so a penalized maximum likelihood estimate approach proposed by Firth was used to obtain parameter estimates (SAS 2011).

Online Resource 2 Literature Cited

SAS (2011) Usage Note 22599: Understanding and correcting complete or quasi-complete separation problems. http://support.sas.com/kb/22/599.html

Online Resource 3

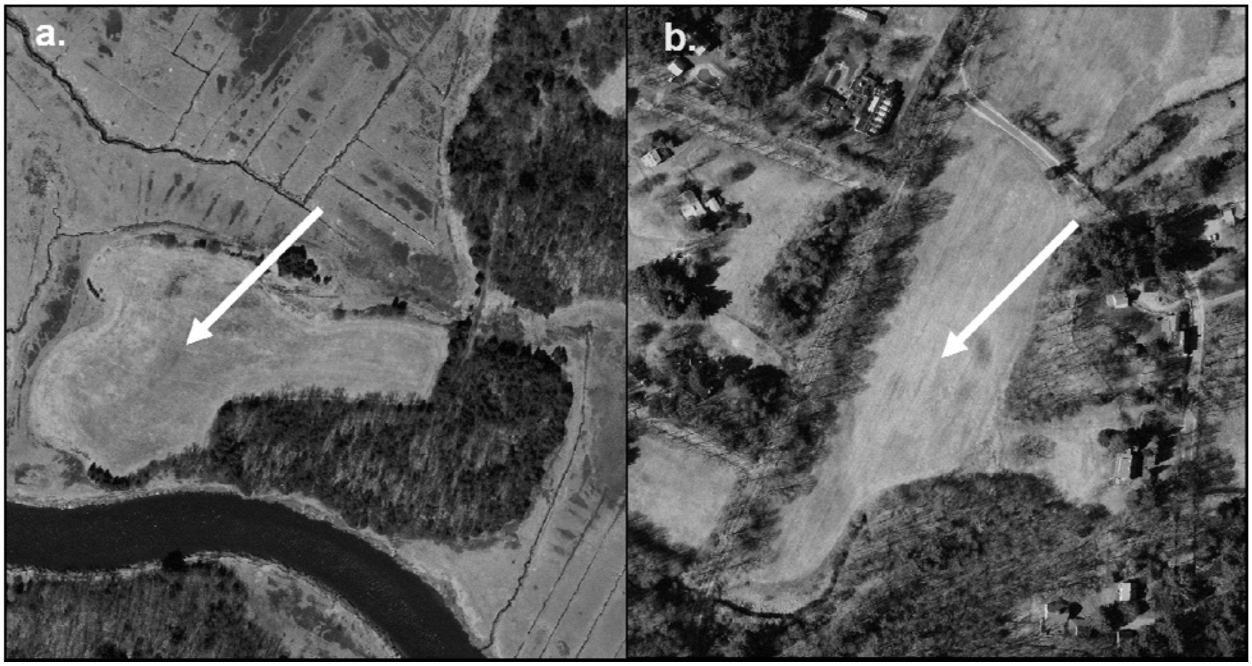

Fig. S3-1 Examples of a small open site (a) and a small closed site (b). The open site is bordered by fewer woods, and contains an edge with low shrubs/trees. In contrast, the closed site is bordered on 3 sides by tall trees. White arrows indicate fields (a. Old Town Hill, Newbury, MA; b. Lower Browning Field, Lincoln, MA). Photographs are 2008 aerial imagery from USGS obtained via MassGIS http://www.mass.gov/mgis/whatis.htm